Prediction of Self-Pressurization Rate of Cryogenic Propellant Tankage

John I. Hochstein* and Hyun-Chul Ji†
Washington University, St. Louis, Missouri
and
John C. Aydelott‡
NASA Lewis Research Center, Cleveland, Ohio

The SOLA-ECLIPSE code is being developed to enable prediction of the behavior of cryogenic propellants in spacecraft tankage. A brief description of the formulations used for modeling heat transfer and for determining the thermodynamic state is presented. Code performance is verified through comparison to experimental data for the self-pressurization of scale-model liquid hydrogen tanks. SOLA-ECLIPSE is used to examine the effect of initial subcooling of the liquid phase on the self-pressurization rate of an on-orbit full-scale liquid hydrogen tank typical for a chemical-propulsion orbit transfer vehicle. The computational predictions show that even small amounts of subcooling will significantly decrease the self-pressurization rate. Further, if the cooling is provided by a thermodynamic vent system, it is concluded that small levels of subcooling will maximize propellant conservation.

Nomenclature

A = cross-sectional area
a = local acceleration
C = specific heat
D = material derivative
F = volume-of-fluid function
g = gravitational field
h = film coefficient
k = thermal conductivity
L = characteristic length
Nu = Nusselt number
n = superscript indicating time level
P = pressure
Q = rate of heat transfer
T = temperature
t = time
V = velocity vector
u,v = x and y velocity components, respectively
x,y = spatial coordinates, Cartesian or axisymmetric (x in radial direction)
β = coefficient of thermal expansion
Γ = coefficient of diffusion
ξ = switching integer: 0, Cartesian; 1, cylindrical
ν = kinematic viscosity
ρ = density

Introduction

IN support of national goals for the exploration of space, a reduced gravity fluid-management technology program has been pursued for over two decades.[1] The purpose of this program is the development of technology required for the design of fluid-management systems to accomplish tasks such as liquid acquisition, thermal control of cryogenic tankage, and fluid transfer. Experimental, analytical, and computational efforts have been integrated as various engineering technologies have developed. The work reported here is focused on the problem of cryogenic propellant tank pressure control.

The high specific impulse available from a liquid-hydrogen-based propulsion system makes it a very attractive option for spacecraft design. Liquid hydrogen has many unusual properties when compared with common liquids that require special attention in the design of both the propulsion system and the associated propellant management system. The low boiling point of hydrogen and the low thermal conductivity of both the gas and liquid phases were of particular interest to our investigation. This combination makes it possible for solar heating to result in the coexistence of subcooled liquid and superheated vapor within the same tank. When such a situation occurs, simple thermodynamic analysis cannot predict accurately the rate of pressure rise within the system.

Early studies focused on the experimental measurement of self-pressurization rates of partially filled spherical tanks. These studies were performed in both 1-g environments[2,3] and low-g environments.[4,5] Experimental data were compared[2-4] to a pressure-rise model based entirely on surface evaporation and to a model based on the assumption of a homogeneous mixture. Neither model provided good predictive capability. Several important physical conclusions were drawn from the data, and these experiments still serve as the primary source of data on liquid hydrogen tankage self-pressurization rates.

The ability to predict pressure-rise rates in actual spacecraft tankage is of obvious importance in vehicle design and mission planning. Various analytical and computational models have been developed to try to meet this need. A finite-difference model[6] that included boiling, convection, and an ideal gas model for the vapor was found to be inadequate when compared with experimental data. Reference 7 compared the predictive capabilities of the Saturn II pressurization program and the REPORTER program. Careful matching of the imposed boundary conditions produced fairly good agreement with experimental data, but the review concluded that both

Received Jan. 1, 1986; revision received Oct. 29, 1988.

*Assistant Professor, Mechanical Engineering. Member AIAA.
†Research Assistant, Mechanical Engineering. Member AIAA.
‡Aerospace Engineer.

models were inadequate with respect to liquid stratification and propellant boiloff. Simple correlations based on curve fits to experimental data have been proposed,[8] but are intended to provide only rough estimates of pressure rise rates.

Although the SOLA-ECLIPSE code (Energy Calculations for LIquid Propellants in a Space Environment) is being developed as a general model for the behavior of cryogenic propellants in spacecraft tankage, the focus here is restricted to its application to the prediction of self-pressurization rates in cryogenic tankage. The starting points for its development were the NASA SOLA-VOF code[9] and the NASA-VOF2D code.[10] A previous version of the SOLA-ECLIPSE code examined the feasibility of jet-induced mixing in cryogenic propellant tanks.[11] The following sections present a brief description of the development of SOLA-ECLIPSE, the numerical results that have been obtained by modeling the previously cited experiments, and the computational predictions of self-pressurization rates for future full-scale orbit transfer vehicle (OTV) liquid hydrogen tanks.

Outline of Baseline Code Capabilities

A family of codes has been developed that use the SOLA algorithm to solve the two-dimensional (Cartesian or axisymmetric) Navier-Stokes equations on an Eulerian mesh of rectangular computational cells. The NASA-VOF2D Code[10] is the newest member of this family and incorporates improved treatment of boundaries that are not aligned with the computational mesh. The code solves the laminar hydrodynamic problem for the primitive variables p, u, and v as stated by the incompressible constant-property Navier-Stokes equations.

$$\frac{\partial u}{\partial x} + \frac{\partial v}{\partial y} = 0 \tag{1}$$

$$\frac{\partial u}{\partial t} + u\frac{\partial u}{\partial x} + v\frac{\partial u}{\partial y} = a_x - \frac{1}{\rho}\frac{\partial p}{\partial x} + \nu\left[\frac{\partial^2 u}{\partial x^2} + \frac{\partial^2 u}{\partial y^2} + \xi\left(\frac{1}{x}\frac{\partial u}{\partial x} - \frac{u}{x^2}\right)\right] \tag{2}$$

$$\frac{\partial v}{\partial t} + u\frac{\partial v}{\partial x} + v\frac{\partial v}{\partial y} = a_y - \frac{1}{\rho}\frac{\partial p}{\partial y} + \nu\left(\frac{\partial^2 v}{\partial x^2} + \frac{\partial^2 v}{\partial y^2} + \frac{\xi}{x}\frac{\partial v}{\partial x}\right) \tag{3}$$

A staggered grid is used with the velocities evaluated at cell faces and pressure defined at cell centers.

The volume-of-fluid (VOF) concept is based on a step function F, which takes on a value of 1 at points in space that are occupied by fluid and a value of 0 at points that are not occupied by fluid. The average value of F for a cell can be used to identify the cell as being full, empty, or a cell through which the free surface passes. Further, the value of F in a free-surface cell, in conjunction with the F-values in its neighbors, can be used to determine the location and curvature of the free surface. The NASA-VOF2D code contains two features that are unique among the family of SOLA codes. The first is the complex model used for computing the free-surface shape and imposing the corresponding surface-tension effects. Although of limited concern for normal gravity problems, surface tension becomes an important phenomena for the analysis of low-g problems. The second is the inclusion of a partial cell treatment for boundaries that are not aligned with the computational mesh.[12]

Heat-Transfer Models

The pressure-rise rate in a liquid hydrogen tank is a function of the rate of heat transfer, the thermodynamic behavior of hydrogen, and the resulting distribution of energy within the tank. Although the baseline codes are capable of solving the hydrodynamic flow problem, they do not contain models for evaluating the thermodynamic behavior or solving the thermal energy equation. The techniques used to solve the thermal transport problem and for evaluating the thermodynamic behavior of the gaseous phase are described in the following sections.

Heat Transfer in Liquid Phase

The heat-transfer model was built on the infrastructure provided by the NASA-VOF2D code. The staggered-grid formulation is retained with the definition of temperature as a cell-centered quantity. The feature added to the code here is a model for thermal energy transport in a propellant inside spacecraft tankage. Since all components in such a system are expected to be at low temperatures, heat transfer by radiant transport has not been included in the computational model.

In evaluating the importance of natural convection processes, it was noted that in the reduced-gravity environment of Earth orbit, they will be greatly inhibited and, for zero-gravity environments, they will be entirely absent. Further, since the driving potential is reduced, the time required to establish a steady-state natural convection flow pattern is substantially greater than under 1-g conditions. One procedure for estimating the time required to establish natural convection in a reduced-gravity environment[18] predicts a transient time of 32 h for a characteristic length of 10 ft and a ΔT of 1°F in an acceleration environment of 10^{-5} g. The issue is further complicated by the effect of heat flux distribution about the tank on the flow patterns established due to natural convection. It has ben found[19] that although bottom heating results in essentially complete mixing, side heating will result in fluid stratification. Therefore, the choice for a thermal energy-transport model is between a detailed natural convection model that couples the momentum equation to the thermal energy equation through a buoyancy term, or a simpler model based on effective conductivity. Since SOLA-ECLIPSE is intended for reduced-gravity applications and the effective conductivity model is simpler and requires significantly fewer computations, it was decided to develop a diffusive transport model that incorporates an effective conductivity.

Applying the foregoing restrictions to an isotropic media results in the following expression for the thermal energy equation:

$$\rho C\frac{\partial T}{\partial t} = \frac{1}{x^{\xi}}\frac{\partial}{\partial x}\left(x^{\xi}\Gamma\frac{\partial T}{\partial x}\right) + \frac{\partial}{\partial y}\left(\Gamma\frac{\partial T}{\partial y}\right) \tag{4}$$

This differential equation has been approximated using finite volume techniques to arrive at the following equation:

$$T^{n+1} = T^n + \frac{\Delta t}{\rho C}(\Sigma \text{ face fluxes}^n) \tag{5}$$

An explicit formulation was chosen because the hydrodynamic formulation is explicit and the long-range goal of the authors is to fully couple all of the various models under development. Equation (5) is enforced for every cell that contains liquid, but not for "empty" cells that contain only vapor. Treatment of the vapor region is described in a later section.

The solution of Eq. (5) requires an evaluation of the generalized diffusion coefficients. For the case of pure conduction, the diffusion coefficient is simply the thermal conductivity k. Since much of the available experimental data was obtained under normal-gravity conditions, it is desirable to model the resulting natural convection in at least a gross sense. An effective conductivity model for the natural convection should serve this purpose. In fact, the use of 1-g data for code verification should emphasize the inadequacies of the model if they are significant. The following simple correlation for natural convection in an enclosure was selected as being representative[13]:

$$Nu_L = 0.0605\left(\frac{L^3 g\beta Pr\Delta t}{\nu^2}\right)^{1/3} \tag{6}$$

The film coefficient resulting from this equation is related to the diffusion coefficient by considering the expression for heat transfer between two adjacent cells based on pure conduction and the use of a film coefficient for convection.

$$\frac{Q}{A} = k\frac{\Delta T}{\Delta x} \quad \text{or} \quad h\Delta T \tag{7}$$

The appropriate effective diffusion coefficient is therefore

$$k_{\text{eff}} = (Nu_L)(k) \tag{8}$$

The remaining task in evaluating the diffusion coefficient is selection of a mixing length scale. For the solid enclosure, it is taken to be the cross-sectional area divided by the wetted perimeter, which corresponds to one-half the radius for a circular cross section. Further, the driving potential is the difference between the wall and bulk temperatures, whereas the driving potential that will be used in evaluating the diffusion coefficient will be based on cell-to-cell temperature variation. The length scale chosen for evaluating the effective conductivity has been selected as one-tenth the radius. This is based on an order-of-magnitude estimate of expected fluid motions. No claim is made that a microscopically accurate model has been constructed, but it is hoped that reasonably good agreement can be obtained on a macroscopic scale. It should be recalled that the main motivation for inclusion of such a model is to permit comparison of code predictions to normal-gravity experimental data, and that the ultimate application of the code is intended to be low-gravity environments where the errors introduced by the effective conductivity model should be small. The expression used to evaluate the diffusion coefficient in the code is

$$\Gamma = k + k_{\text{eff}} \tag{9}$$

This form permits calculations in both normal- and low-gravity environments without the need for changing models.

Imposition of appropriate boundary conditions is the only issue to be resolved in order to complete the thermal analysis of the liquid phase. The appropriate on-orbit boundary condition is a specified heat flux to the tank. Furthermore, the experimental data that will be used to verify code performance were also collected using a known heat flux boundary condition. The formulation given by Eq. (5) is particularly well suited for the imposition of such a boundary condition by the insertion of the appropriate flux term. The question of an appropriate boundary condition at the free surface is addressed in a later section.

Heat Transfer in the Gaseous Phase

The vapor region is modeled as a single node that is connected to the tank walls and to each free-surface cell. The gas is assumed to be well mixed and in quasistatic thermodynamic equilibrium. The heat-transfer calculations therefore reduce to computing the heat flux to and from the node and relating it to the internal energy of the gas. The heat transfer from the tank walls is computed by simply multiplying the specified flux by the tank surface area exposed to the gas. This rate is integrated over time to obtain a total internal energy and a corresponding temperature. Modeling the heat transfer between the gaseous phase and the liquid is described in the following section.

Heat Transfer at the Free Surface

Heat transfer to and from free-surface cells poses special difficulties. Since the geometric center of a surface cell can no longer be assumed to be the center of mass of the cell, the meaning of a temperature value and details of its calculation must be re-evaluated. The code executes a complex series of tests and calculations to determine 1) the orientation of the surface within the cell, 2) the area of the surface within the cell, 3) the center of mass of the liquid within the cell, and 4) the distances from the center of mass to the center of mass of neighbor cells that also contain liquid. The definition of temperature as a cell-centered quantity has been refined to mean the temperature at the center of mass of the cell. The two definitions are entirely consistent for full cells. The revised center-to-center differences are used in evaluating the flux terms for heat transfer between cells containing liquid.

Heat transfer between the liquid and gas phases must be accounted for when performing an energy balance for a surface cell. Since the gas phase is modeled as a single node, an appropriately simple expression for interphase heat transfer was sought. The transport due to evaporation or condensation has been accounted for in the thermodynamic behavior model, which will be described later. The remaining interphase transport has been modeled by a gradient diffusion process. The driving potential is the difference between the gas-node temperature and surface-cell temperature. The length scale is assumed to be one-tenth the radius of the tank, and the diffusion coefficient is the thermal conductivity of the gas.

Thermodynamic Model

Physical Properties

The vapor phase was assumed to be in quasistatic thermodynamic equilibrium. Evaluation of the conditions expected for liquid cryogenic tankage showed that the thermodynamic state of the vapor would not be sufficiently far removed from the critical point to justify use of the ideal gas model. Since our specific interest here was tank self-pressurization, and the pressure is highly dependent on the thermodynamic model for the vapor phase, it was decided that a more accurate model than the ideal gas assumption would be required.

The thermodynamic model in SOLA-ECLIPSE is based on the integration of Maxwell's equations using curve fits of the thermodynamic data. A good description of the concepts behind this procedure is provided in Ref. 14. A set of subroutines have been written to perform the required calculations, and they are accessed through external function calls. The subroutine system has been structured so that any pair of thermodynamic properties can be submitted to the system, and the system will return values for all other thermodynamic properties of interest. For the tank pressure-rise problem, the two known quantities are enthalpy and density. The enthalpy is determined by the thermal energy balance described in the previous section. The density is known since the initial mass in the vapor region is uniquely determined by the specified initial conditions, and any mass additions or deletions due to phase change are tracked by the procedures described in the following sections. Submission of these two values to the thermodynamic model will result in the return of values for properties such as gas pressure and saturation temperature. The model includes statements that terminate calculations if one of the properties drifts out of the range for which the model is applicable.

Evaporation and Boiling

A serious shortcoming of some previous models was the lack of a capability to account for phase change. Heat transfer from superheated vapor to the liquid surface is likely to cause evaporation. Even though heat flux to on-orbit tankage is expected to be relatively low, the lack of strong natural convection mechanisms combined with the low thermal conductivity of the liquid may well lead to local hot spots and, therefore, to boiling. Since the density ratio of the phases is approximately 70 to 1, even a small amount of phase change will have a significant impact on the pressure-rise rate.

Phase change is accounted for on a cell-by-cell basis. After the thermal energy balance calculations have been performed, the temperature in each cell is compared to the saturation temperature corresponding to the current pressure. If the temperature of a free-surface cell exceeds the saturation tempera-

ture, the heat of vaporization is used to compute the amount of mass that must undergo evaporation in order to reduce the cell temperature to the saturation temperature. This mass is then deleted from the cell and added to the vapor region. For a cell containing a solid boundary, evaluation of boiling is accomplished in a similar manner. The only additional consideration is the level of superheat required to initiate boiling. Published data for incipient boiling of hydrogen are limited, and published values range from 0.1 to 3.0°F.[20,21] A value of 0.5 K was selected as representative of the published data. Therefore, the computational procedure requires that the cell temperature exceed saturation by 0.5 K before vaporization is initiated. Although it is likely that for the case of local boiling some of the vapor will condense before reaching the vapor region, the assumption used in the code is conservative since it should result in higher than actual self-pressurization rates.

Computational Results for Model Tanks

The first cases to be modeled were the normal-gravity self-pressurization experiments reported in Ref. 2. The computational mesh used to analyze this case is shown in Fig. 1 superimposed over a partially filled tank. One of the conclusions drawn by this study was that the pressurization rate was dependent on "the location of the heat addition relative to the liquid location." For this reason, three test cases were selected from among those presented in the report. The first was for a uniform heating test, the second for a bottom heating test, and the third for a top heating test. In like sequence, Figs. 2–4 present a comparison of experimental results for these cases with computational predictions. Although the uniform heating and bottom heating cases show excellent agreement, the initial pressure-rise rate was overpredicted, and the later pressurization rate underpredicted for the top heating case. It is believed that this is due to inadequacies in the interfacial model coupling the gas and liquid phases. During the initial period, insufficient heat transfer across the interface may lead to overprediction of the pressurization rate. During the later period, use of an effective conductivity in the liquid phase will overpredict mixing since top heating will promote thermal stratification rather than establish convection patterns. Overenhanced mixing will underpredict liquid surface temperature, thereby suppressing evaporation at the free surface and underpredicting the pressurization rate late in the test. It should be noted that these three cases as well as the cases cited next all extend to pressure levels considerably higher than those expected in actual cryogenic tankage.

The second tank to be modeled was the spherical tank of Ref. 3 that was used to examine the effect of size on self-pressurization rates in normal gravity. Figure 5 presents a comparison of the code predictions to the experimental data. Again, the pressure-rise rate is slightly overpredicted.

The final experimental case to be modeled was the low-gravity test reported in Ref. 4. This experiment used the same spherical container as the first three cases modeled, but was executed in an acceleration environment of approximately 10^{-3} g's. This is the test case most representative of the actual conditions for which the predictive capability is being developed. Figure 6 presents a comparison of experimental data to computational predictions. Although the pressure-rise rate is slightly underpredicted, the agreement with the experimental data is quite good.

Before drawing conclusions about the accuracy of SOLA-ECLIPSE, an honest evaluation requires reporting of the failures encountered in modeling experimental data. When cases were run with a large heat flux, the predicted pressure rise was not only larger than actual but diverged from the experimental

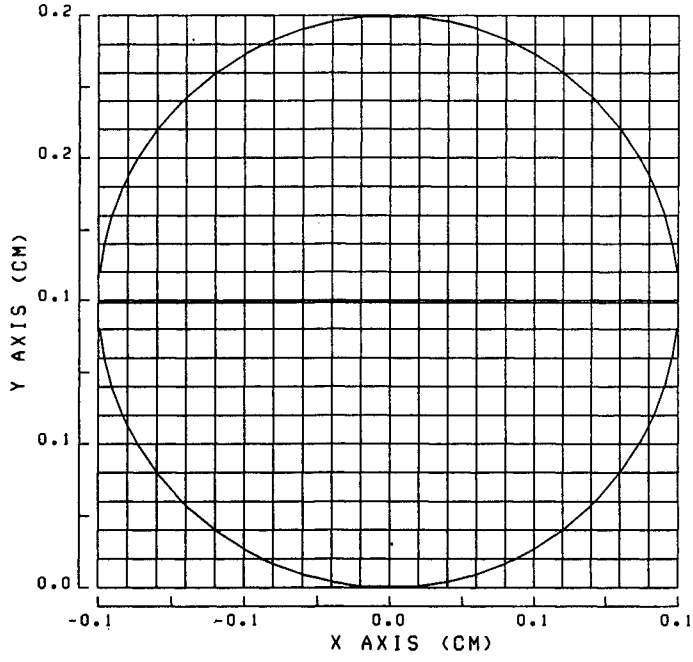

Fig. 1 Computational mesh for model tanks.

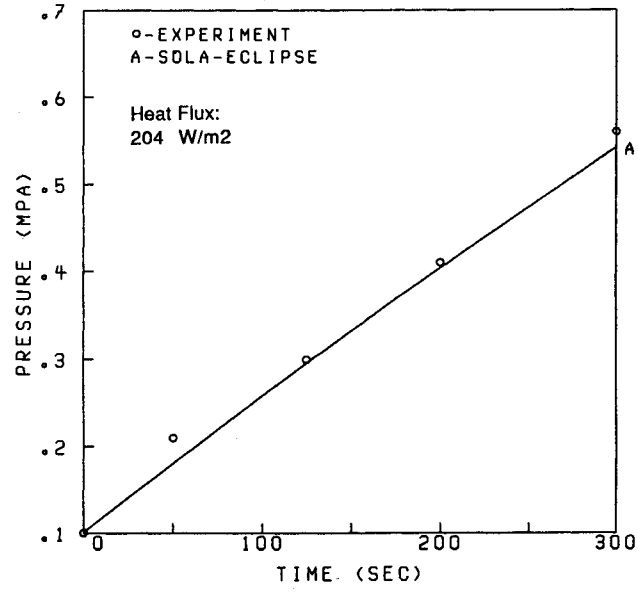

Fig. 2 Self-pressurization rate, uniform heating (diam = 23 cm, 1 *g*).

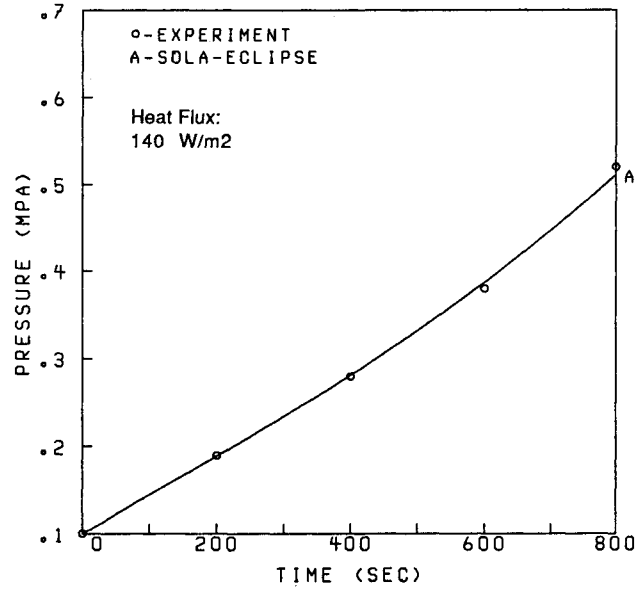

Fig. 3 Self-pressurization rate, bottom heating (diam = 23 cm, 1*g*).

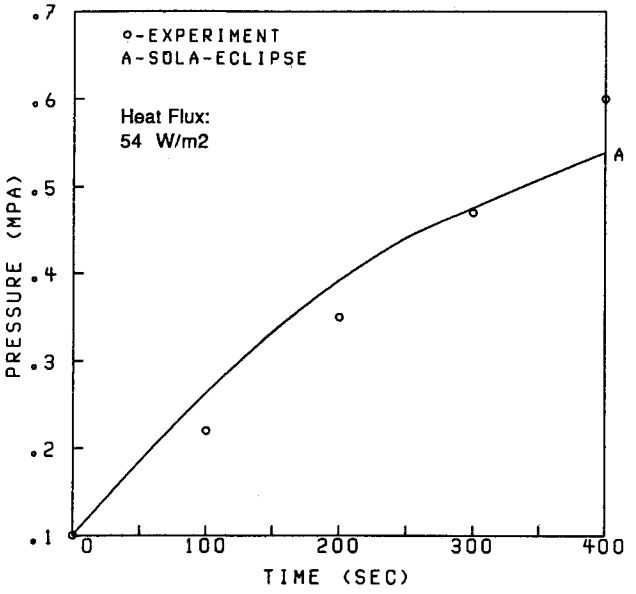

Fig. 4 Self-pressurization rate, top heating (diam = 23 cm, 1 *g*).

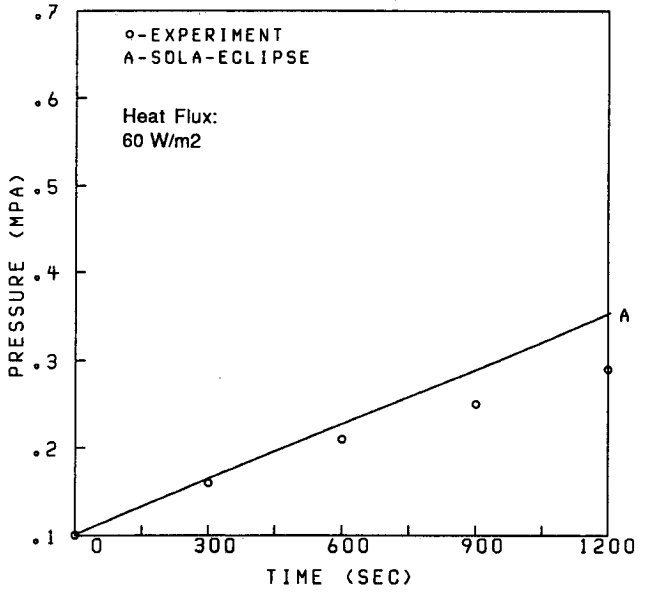

Fig. 5 Self-pressurization rate, uniform heating (diam = 56 cm, 1 *g*).

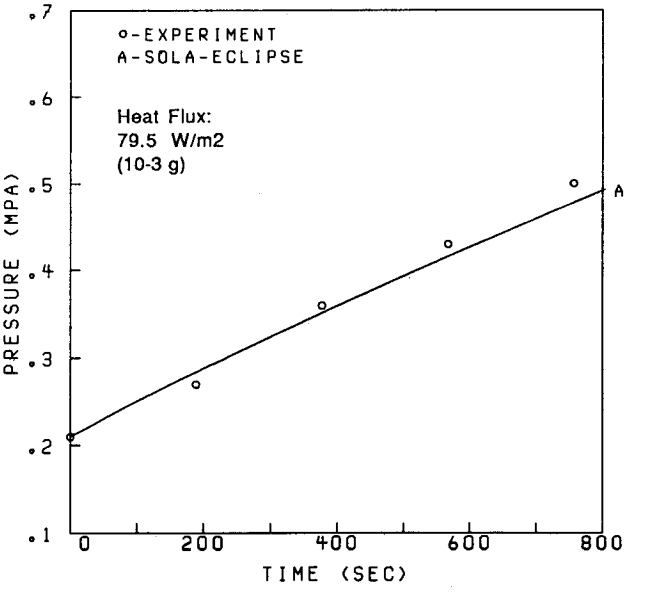

Fig. 6 Self-pressurization rate, uniform heating (diam = 23 cm, low gravity).

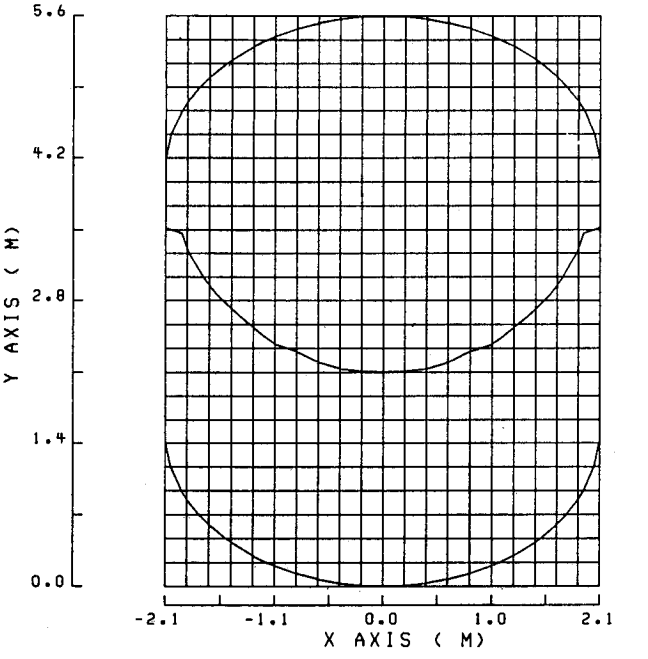

Fig. 7 Computational mesh for OTV tanks.

results as time progressed. Examination of the detailed code operation revealed that a large amount of boiling was being predicted and that the mass addition to the vapor phase was causing a rapid pressure rise. Boiling, the associated liquid mixing, and subsequent bubble collapse are not well modeled by the code. It must be concluded that this code will be inadequate for high heat flux cases. Since heat flux rates experienced by on-orbit tankage are actually lower than for the cases successfully modeled, the inability to model high flux situations is not a significant drawback.

Based on the evidence presented in the preceding paragraphs, it was concluded that the SOLA-ECLIPSE code is a viable tool for predicting the on-orbit self-pressurization rate of cryogenic propellant tankage.

Computational Results for Full-Scale On-Orbit Tanks

Previous studies[11,15] have examined the feasibility of actively mixing the liquid phase by the introduction of a mixing jet into the pool of liquid. The motivation for inducing such mixing is to suppress evaporation and boiling and to thereby suppress the pressure-rise rate. This is accomplished by extracting a small amount of fluid from the tank, cooling it, and reinjecting it as a jet to help distribute the cooling effect throughout the tank. Since the cooling will require an expenditure of energy, it is highly desirable to identify what level of subcooling would be optimal for such a system. The parametric study reported in the following paragraphs assumes the mixing process is already complete and a uniform temperature stagnant field is taken as an initial condition. The study seeks to answer the question: For a partially full tank of stagnant liquid hydrogen in Earth orbit, does initial subcooling of the liquid affect the self-pressurization rate, and if so, what is the affect of different levels of subcooling?

The tank chosen for this study is the liquid hydrogen tank for a "typical" chemical-propulsion OTV.[16] The dimensions given in the reference were slightly modified to facilitate code debugging. The computational mesh used to model the problem is presented in Fig. 7, superimposed over a partially full tank. The barrel section has a radius of 2.1 m and a length of 2.6 m. The heads are elliptical with a semiminor axis of 1.5 m

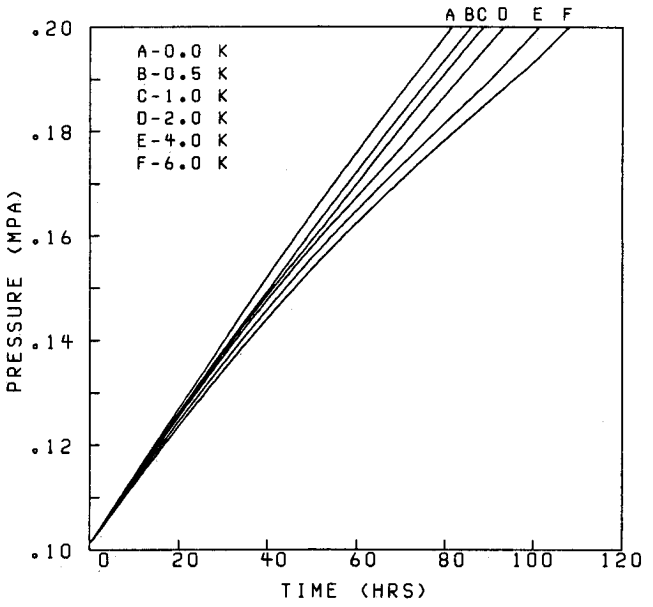

Fig. 8 Pressure rise in OTV tank (50% full).

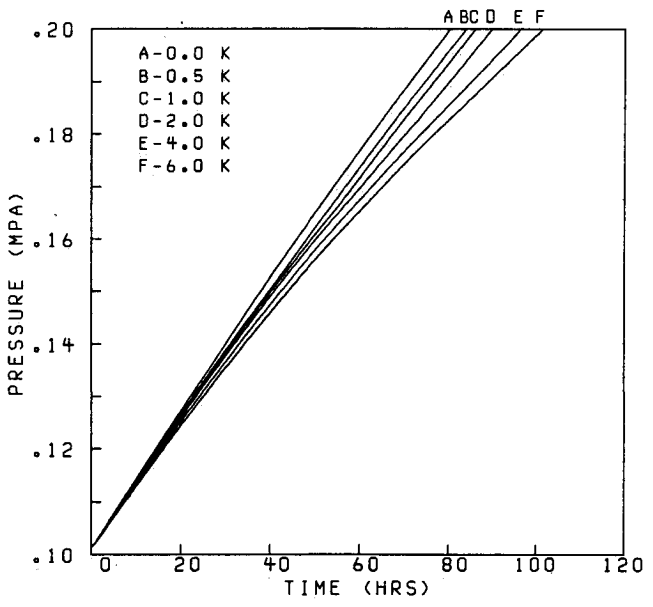

Fig. 9 Pressure rise in OTV tank (40% full).

in length. Two parameters were selected for variation during the study: degree of initial subcooling and tank filling. The heat flux to the tank was specified as 1.3 W/m^2 for all test cases. This is a typical value used by NASA personnel in computing heat transfer to vehicles in Earth orbit.[17] Because of the desirability of lightweight tanks, a pressure of 0.2 mPa (approximately 2 atm) was selected as the termination point for the analyses. The maximum level of initial subcooling selected for analysis was 6 deg because this corresponds to the minimum liquid temperature likely to be obtained by currently proposed cooling devices.

The predicted self-pressurization rates are presented in Figs. 8–11 for tank fillings of 50, 40, 30, and 20%, respectively. Each figure displays predicted pressure-rise rates based on five different levels of initial subcooling of the liquid phase: 0.0, 0.5, 2.0, 4.0, and 6.0 K. Such levels of subcooling appear to be obtainable through the combination of a thermodynamic vent system with jet-induced mixing.[11] It should be noted that reduction in size of these figures has decreased the apparent curvature of the pressure vs time curves. When viewed in a full-page format, even the zero subcool case results in the noticeable curvature of the pressure history curve.

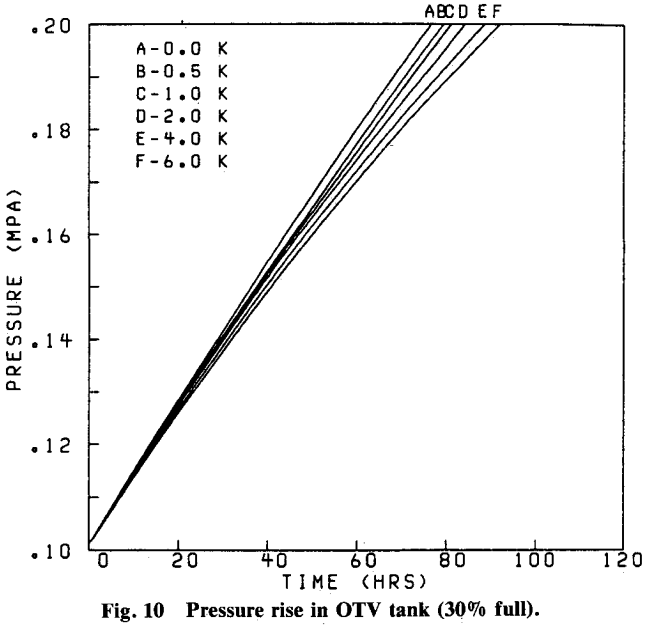

Fig. 10 Pressure rise in OTV tank (30% full).

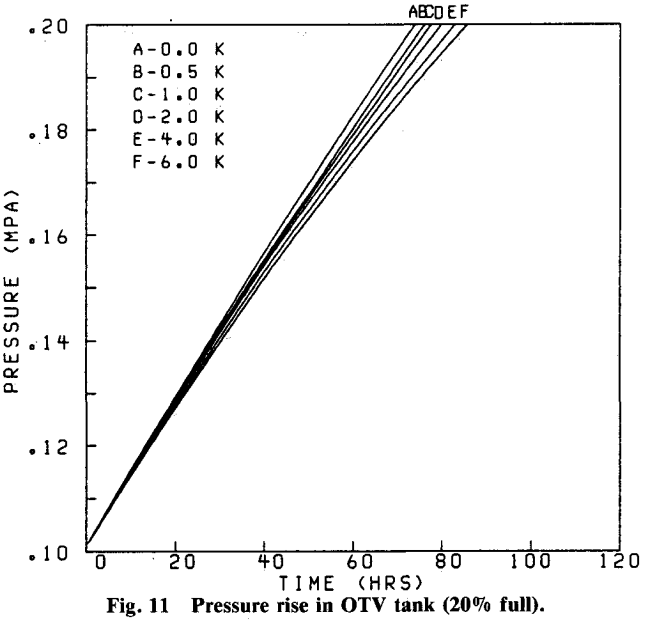

Fig. 11 Pressure rise in OTV tank (20% full).

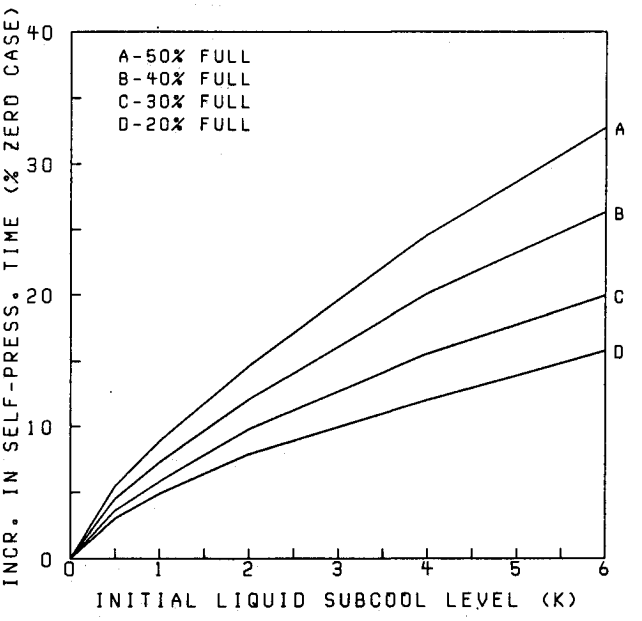

Fig. 12 Effectiveness of subcooling.

A review of Figs. 8–11 shows that increases in the amount of initial subcooling extend the length of time required for the internal tank pressure to rise from atmospheric pressure to 0.2 mPa. This effect is more pronounced for the larger fillings, but is still significant for the 20% full case. Figure 12 presents a comparison of the percent increase in elapsed time for self-pressurization (to 0.2 mPa) to the amount of initial subcooling of the liquid phase. This figure indicates that the relationship between initial subcool level and self-pressurization rate is not linear. Rather, the effectiveness of incremental increases in the subcool level diminishes with increasing levels of subcooling. If we assume that the amount of subcooling is directly proportional to the amount of fluid expended in a TVS, a small amount of subcooling appears to maximize conservation of propellant.

Concluding Remarks

The SOLA-ECLIPSE code has been used to predict the self-pressurization rates of scale-model liquid hydrogen tanks for which experimentally measured data were available. Cases analyzed include both normal-gravity and low-gravity environments and both uniform and nonuniform heating of the tank. In all cases, there is either good agreement between predicted and measured values or the computations overpredict the self-pressurization rate. It should be noted that the heat fluxes for these cases are at least an order of magnitude larger than expected for an actual orbiting vehicle. In particular, the low-gravity cases were restricted to high heat fluxes due to the limited time available for execution of an experiment in a low-gravity environment.

Based on the comparison of predicted to measured self-pressurization rates in scale-model tanks, SOLA-ECLIPSE is judged capable of predicting self-pressurization rates in cryogenic propellant tanks. Prediction of self-pressurization rates for full-scale on-orbit OTV tanks has been performed using the SOLA-ECLIPSE code. The amount of initial subcooling of the liquid phase has been shown to significantly affect the self-pressurization rate of partially filled tanks. Even a small degree of initial subcooling (0.5 K) will have a significant impact. Examination of detailed code output reveals that this small amount of subcooling is sufficient to delay evaporation at the gas-liquid interface and therefore lower the self-pressurization rate. It is also interesting to note that a small amount of boiling is predicted for almost all cases near the end of the analyses. The most dramatic suppression of self-pressurization rate was accomplished for a 50% full tank with an initial subcooling of 6 K. When this case is compared to self-pressurization initiated from saturated conditions, there is a 33% increase in the time required for self-pressurization from one atmosphere to 0.2 mPa.

Based on the computational prediction of self-pressurization rates for full-scale on-orbit OTV tanks by the SOLA-ECLIPSE code, the self-pressurization rate of on-orbit cryogenic tankage can be significantly decreased by initial subcooling of the liquid phase. The maximum conservation of propellant appears to be achieved with a small level of subcooling.

Acknowledgment

This work was supported by the NASA Lewis Research Center through Grant NAG3-578 with John C. Aydelott as the Technical Officer.

References

[1]Aydelott, J. C., Carney, M. J., and Hochstein, J. I., "NASA Lewis Research Center Low-Gravity Fluid Management Technology Program," AIAA Paper 85-002, Nov. 1985.

[2]Aydelott, J. C., "Normal Gravity Self-Pressurization of 9-Inch Diameter Spherical Liquid Hydrogen Tankage," NASA TN-D-4171, Oct. 1967.

[3]Aydelott, J. C., "Effect of Size on Normal Gravity Self-Pressurization of Spherical Hydrogen Tankage," NASA TN-D-5196, May 1969.

[4]Abdalla, K. L., Frysinger, T. C., and Andracchio, C. R., "Pressure Rise Characteristics for a Liquid-Hydrogen Dewar for Homogeneous, Normal-Gravity Quiescent, and Zero-Gravity Tests," NASA TM-X-1134, Sept. 1965.

[5]Aydelott, J. C., "Effect of Gravity on Self-Pressurization of Spherical Liquid Hydrogen Tankage," NASA TN-D-4286, Dec. 1967.

[6]Merte, H. et al., "Transient Pressure Rise of a Liquid-Vapor System in a Closed Container Under Variable Gravity," 4th International Heat Transfer Conference, Paris, France, Sept. 1970.

[7]Bradshaw, R. D. et al., "Evaluation and Application of Data from Low-Gravity Orbital Experiment," General Dynamics/Convair, GDC-DDB70-003, April 1970.

[8]Blatt, M. H., "Empirical Correlations for Pressure Rise in Closed Cryogenic Containers," *Journal of Spacecraft and Rockets*. Vol. 5, June 1968, pp. 733–735.

[9]Hotchkiss, R. S., "Simulation of Tank Draining Phenomena with the NASA SOLA-VOF Code," Los Alamos Scientific Laboratory, Los Alamos, New Mexico, Rept. LA-8168-MS, 1979.

[10]Torrey, M. D., Cloutman, L. D., Mjolsness, R. C., and Hirt, C. W., "NASA-VOF2D: A Computer Program for Incompressible Flows with Free Surfaces," Los Alamos Scientific Laboratory, Los Alamos, New Mexico, Rept. LA-10612-MS, 1985.

[11]Hochstein, J. I., Gerhart, P. M., and Aydelott, J. C., "Computational Modeling of Jet Induced Mixing of Cryogenic Propellants in Low-g," AIAA Paper 84-1344, June 1984.

[12]Hirt, C. W. and Sicilian, J. M., "A Porosity Technique for the Definition of Obstacles in Rectangular Cell Meshes," Flow Science Rept. FSI-85-00-5, Sept. 1985.

[13]Chapman, A. J., *Heat Transfer,* 4th ed. Macmillan, New York, 1984, p. 391.

[14]Reynolds, W. C., *Thermodynamic Properties in SI,* Dept. of Mech. Eng., Stanford Univ., 1979.

[15]Aydelott, J. C., "Axial Jet Mixing of Ethanol in Cylindrical Containers During Weightlessness," NASA TP-1487, July 1979.

[16]Blatt, M. H., Bradshaw, R. D., and Risberg, J. A., "Capillary Acquisition Devices for High Performance Vehicles, Executive Summary," General Dynamics/Convair, GDC-CRA-80-003, 1980 (also NASA CR-159658).

[17]Cramer, T., Brogen, E., and Siegel, B., "Evaluation of Propellant Tank Insulation Concepts for Low Thrust Chemical Propulsion Systems," Boeing Aerospace Co., NASA CR-168320, March 1984.

[18]Adelberg, M. and Schwartz, S. H., "Heat Transfer Domains for Fluids in a Variable Gravity Field with Some Applications to Storage of Cryogens in Space," *Advances in Engineering,* Vol. 11, edited by K. D. Timmerhaus, Plenum, New York, 1965, 568–583.

[19]Tatom, J. W., Brown, W. H., Knightr, L. H., and Coxe, E. F., "Analysis of Thermal Stratification of Liquid Hydrogen in Rocket Propellant Tanks," *Advances in Cryogenic Engineering,* Vol. 9, edited by K. D. Timmerhaus, Plenum, New York, 1963, pp. 265–272.

[20]Sherley, J. E., "Nucleate Boiling Heat Transfer Data for Liquid Hydrogen at Standard and Zero Gravity," *Advances in Cryogenic Engineering,* Vol. 8, edited by K. D. Timmerhaus, Plenum, New York, 1963, pp. 495–500.

[21]Drayer, D. E. and Timmerhaus, K. D., "An Experimental Investigation of the Boiling and Condensation Heat Transfer Coefficient for Hydrogen," *Advances in Engineering,* Vol. 7, edited by K. D. Timmerhaus, Plenum, New York, 1962, pp. 401–412.